Tryptophanyl Adenylate Formation by Tryptophanyl-tRNA Synthetase from *Escherichia coli*†

Michel Merle,* Veronique Trezeguet, Pierre Vincent Graves, David Andrews, Karl H. Muench,‡ and Bernard Labouesse

Institut de Biochimie Cellulaire et Neurochimie, CNRS, F33077 Bordeaux, France

Received July 12, 1985

ABSTRACT: By gel filtration and titration on DEAE-cellulose filters we show that *Escherichia coli* tryptophanyl-tRNA synthetase forms tryptophanyl adenylate as an initial reaction product when the enzyme is mixed with ATP–Mg and tryptophan. This reaction precedes the synthesis of the tryptophanyl-ATP ester known to be formed by this enzyme. The stoichiometry of tryptophanyl adenylate synthesis is 2 mol per mole of dimeric enzyme. When this reaction is studied either by the stopped-flow method, by the fluorescence changes of the enzyme, or by radioactive ATP depletion, three successive chemical processes are identified. The first two processes correspond to the synthesis of the two adenylates, at very different rates. The rate constants of tryptophanyl adenylate synthesis are respectively 146 ± 17 s^{-1} and 3.3 ± 0.9 s^{-1}. The third process is the synthesis of tryptophanyl-ATP, the rate constant of which is 0.025 s^{-1}. The Michaelis constants for ATP and for tryptophan in the activation reaction are respectively 179 ± 35 μM and 23.9 ± 7.9 μM, for the fast site, and 116 ± 45 μM and 3.7 ± 2.2 μM, for the slow site. No synergy between ATP and tryptophan can be evidenced. The data are interpreted as showing positive cooperativity between the subunits associated with conformational changes evidenced by fluorometric methods. The pyrophosphorolysis of tryptophanyl adenylate presents a Michaelian behavior for both sites, and the rate constant of the reverse reaction is 360 ± 10 s^{-1} with a binding constant of 196 ± 12 μM for inorganic pyrophosphate (PP_i). Major differences appear between tryptophanyl-tRNA synthetases from *E. coli* and from beef. In the procaryotic enzyme, the two subunits present nearly half-of-the-sites reactivity but exhibit kinetic positive cooperativity toward tryptophan. In the eucaryotic enzyme, the two subunits are identically active at substrate saturation but exhibit negative cooperativity toward tryptophan. The bacterial enzyme makes tryptophan derivatives such as tryptophanamide. The mammal enzyme does not. The *E. coli* enzyme does not cross-react with antibodies raised against the beef protein.

Tryptophanyl-tRNA synthetases, both from *Escherichia coli* and from beef pancreas, are α_2 dimeric proteins (Joseph & Muench, 1971; Gros et al., 1972; Kisselev et al., 1979). The subunits of the procaryotic enzyme have a molecular mass of 37 kDa (Hall et al., 1982) and are among the smallest in the synthetase series. The subunits of the eucaryotic proteins are larger, 54–60 kDa (Lemaire et al., 1969; Favorova et al., 1974), although limited proteolysis can bring their molecular weight down to that of the bacterial enzyme (Lemaire et al., 1975; Prasolov et al., 1975; Scheinker et al., 1979). Such proteolysis destroys the catalytic properties of the beef enzyme, except for the ability to hydrolyze the aminoacyl-tRNA (Epely et al., 1976). The total peptide sequence of this eucaryotic protein seems necessary for its full activity.

There are presently no data on the three-dimensional structure of either *E. coli* or beef tryptophanyl-tRNA synthetases. However, the *Bacillus stearothermophilus* enzyme, which has the same molecular weight and the same subunit composition as the *E. coli* protein (Winter & Hartley, 1977; Coleman & Carter, 1984) and which has common catalytic features (Atkinson et al., 1979), has recently been described in crystalline form (Carter & Carter, 1979). The amino acid sequences of both bacterial synthetases present regions of extensive homology (Hall et al., 1982; Winter & Hartley, 1977), and most probably, these two procaryotic synthetases will be shown to have very close structural and catalytic properties. The sequence of the beef enzyme is currently under determination (J. Bonnet, personnal communication).

Both the *E. coli* and the beef enzymes bind 2 mol of tryptophan per dimer. The subunits of the procaryotic synthetase bind the amino acid with the same affinity (K_d = 120 μM; Muench, 1976) while those of the eucaryotic synthetase exhibit anticooperative binding of this substrate (K_d = 1 and 20 μM; Graves et al., 1979). Both subunits of the beef enzyme are active during the activation (Graves et al., 1980; Mazat et al., 1982). The active site stoichiometry of the bacterial enzyme is not established in the adenylate synthesis.

Apart from aminoacylating its specific tRNA, the *E. coli* enzyme can carry out the synthesis of the tryptophanyl-ATP ester (Muench, 1969; Andrews et al., 1985) as does the *B. stearothermophilus* enzyme (Coleman & Carter, 1984). Moreover, the *E. coli* enzyme can synthesize tryptophanamide (Andrews et al., 1985). The bovine enzyme is also known to produce the tryptophanyl-ATP ester (Weiss et al., 1959), but too slowly to do it significantly under the fast kinetic conditions used to study the aminoacyl adenylate formation (Mazat et al., 1982; Merle et al., 1984). The bovine enzyme does not produce tryptophanamide (Merle, unpublished results). In the *E. coli* system, gel filtration experiments lead to the isolation of a tryptophanyl-ATP–enzyme complex instead of the usual trytophanyl adenylate–enzyme complex (Muench, 1969).

Little information is available on the initial steps of the reactions catalyzed by the *E. coli* enzyme. From what is presently known, three to four successive processes are evi-

† This work was supported by grants from the Centre National de la Recherche Scientifique, the University of Bordeaux II, and the Fondation pour la Recherche Medicale.

‡ Present address: Division of Genetic Medicine, University of Miami School of Medicine, Miami, FL 33101.

0006-2960/86/0425-1115$01.50/0

denced when this enzyme is mixed with ATP and tryptophan in the absence of tRNA (Andrews et al., 1985), while only one is evidenced in the eucaryotic system at substrate saturation (Merle et al., 1984).

Therefore, from gross structural and kinetic standpoints, most properties of the two homologous synthetases appear different. In order to compare the pre-steady-state behavior of the *E. coli* enzyme with that of the beef enzyme and to complement the structural data that are likely to appear on the bacterial enzyme, we have undertaken a study of the early steps of the reactions catalyzed by *E. coli* tryptophanyl-tRNA synthetase, in the absence of tRNA. Rapid kinetic experiments were carried out under either constant or decreasing substrate concentrations. This work was particularly aimed at defining whether the two fast processes preceding the formation of the tryptophanyl-ATP ester correspond to the synthesis of tryptophanyl adenylate and at defining the relative catalytic activities of the two subunits of this enzyme. The information obtained shows that the procaryotic and eucaryotic homologous tryptophanyl-tRNA synthetases exhibit strikingly different kinetic behaviors in the adenylation reaction.

Materials and Methods

Enzymes. Tryptophanyl-tRNA synthetase from *E. coli* was prepared according to Joseph & Muench (1971). Inorganic pyrophosphatase (500 units/mg) was from Sigma.

Labels. L-[^{14}C]Tryptophan (58 Ci/mol) and [^{14}C]ATP (573 Ci/mol) were from Amersham International; ^{32}P-labeled inorganic pyrophosphate ([^{32}P]PP$_i$; 3.5 Ci/mmol) was from New England Nuclear. [β,γ-^{32}P$_2$]ATP was prepared from [^{32}P]PP$_i$–ATP isotopic exchange as follows: 10 mM ATP, 100 μM [^{32}P]PP$_i$, 10 μM tryptophan, and 100 nM bovine tryptophanyl-tRNA synthetase [prepared as in Merault et al. (1978)] were incubated for 4 h at 25 °C in 20 mM potassium phosphate buffer, pH 8.0, containing 10 mM dithioerythritol, 100 μM ethylenediaminetetraacetic acid (EDTA), and 10 mM magnesium acetate. [β,γ-^{32}P$_2$]ATP was used at the indicated concentration (see the text) without any further purification.

Standard Buffer. All experiments were performed in a standard buffer solution containing 100 mM tris(hydroxymethyl)aminomethane hydrochloride (Tris-HCl), pH 8.0, 0.1 mM EDTA, 1 mM dithioerythritol, and 1 mM free magnesium as in Merle et al. (1984).

Gel Filtration of Tryptophanyl-tRNA Synthetase Complexes. Reaction mixtures (200 μL), containing the various reactants at the indicated concentrations, were filtered through a Sephadex G-25 superfine column (0.8 × 25 cm) at 4 °C. The eluent was either the standard buffer or the standard buffer containing 0.4 mM PP$_i$. The flow rate was 10 mL/h. Aliquots (100 μL) of the collected fractions were absorbed onto Whatman 3MM paper disks and then dried. ^{14}C radioactivity was determined by counting the paper disks in 10 mL of toluene Omnifluor scintillator; ^{32}P radioactivity was determined by direct Cherenkof effect.

[^{32}P]PP$_i$–ATP Exchange Kinetics. The exchange reaction was started by adding 10 μL of enzyme solution to 490 μL of the exchange medium in the standard buffer at 25 °C; the final concentrations were 20 nM enzyme, 5 μM tryptophan, 500 μM ATP, and 100 μM [^{32}P]PP$_i$. At 15, 30, and 45 s, 100-μL aliquots were removed and flushed in 200 μL of 5% trichloroacetic acid to stop the reaction. Then, 500 μL of a 3% suspension of activated Norit A charcoal in 5% trichloroacetic acid containing 0.2 M sodium pyrophosphate was added to each sample. After filtration of the mixture through Whatman GF/c filters and washing, the radioactivity retained by the charcoal was counted. A similar procedure was used to determine the [β,γ-^{32}P$_2$]ATP concentration in the [β,γ-^{32}P$_2$]ATP depletion experiments.

Stoichiometry of Tryptophanyl Adenylate Synthesis Determined by Absorption of the Tryptophanyl-tRNA Synthetase Complexes on DEAE-cellulose Filters. Reaction mixtures (500 μL), containing tryptophanyl-tRNA synthetase, inorganic pyrophosphatase, L-[^{14}C]tryptophan, or ATP–Mg at the indicated concentrations, were incubated at 25 °C. Two minutes after each addition of 2 μL of a stock solution of the variable substrate, (ATP–Mg or L-[^{14}C]tryptophan), 10-μL aliquots were removed and absorbed on DEAE-cellulose filters prerinsed with the standard buffer. The filters were washed at 4 °C with 4 mL of precooled standard buffer, then dried, and counted for radioactivity as above. Because of the poor retention of the enzyme on the filters, small volumes of washing solution were used. As a consequence, there was residual radioactivity from free L-[^{14}C]tryptophan. Independent experiments, performed in the absence of enzyme, were carried out in order to correct the contaminant radioactivity from free L-[^{14}C]tryptophan.

Fluorescence Measurements. An Aminco SPF 500 fluorometer was used with a 0.4 × 1.0 cm quartz cell and an excitation path length of 0.4 cm. The excitation wavelength was set at 290 nm, with a 2-nm band-pass, and the emission wavelength was 330 nm, with a 8-nm band-pass.

Stopped-Flow Kinetics. Rapid mixing experiments were performed with a Durrum-Gibson stopped-flow apparatus (dead time, 5 ms). The excitation wavelength was set at 295 nm with a 15-nm band-pass, and the fluorescence emission light was observed after passing through a Corning CS 0.54 filter. The fluorescence signal was recorded as a function of time as 3000 points with a Hewlett-Packard 3437 system voltmeter connected to a Hewlett-Packard 9845 microcomputer, which performed the signal averaging, the original 3000 points being reduced to 168. For each set of reagent concentrations, five to ten stopped-flow runs were accumulated. Fitting of the data was performed with the microcomputer.

Stopped-flow kinetics of adenylate pyrophosphorolysis were performed with a (tryptophanyl adenylate)$_2$–tryptophanyl-tRNA synthetase complex preformed as follows: 2 μM enzyme, 5 μM tryptophan, 20 μM ATP–Mg, and 0.5 unit/mL inorganic pyrophosphatase were incubated for 5 min in standard buffer at 25 °C. Prior to filling the reservoir syringes of the stopped-flow apparatus, 100 mM sodium fluoride was added to the enzyme solution in order to inhibit inorganic pyrophosphatase during the pyrophosphorolysis reaction.

Nonlinear Regression Analysis of Substrate Depletion Experiments. The iterative procedure used was that described by Merle et al. (1984) for depletion kinetics experiments. In the case of the [β,γ-^{32}P$_2$]ATP depletion experiments, the ATP concentration was measured instead of the fluorescence intensity. Fitting of the experimental points was performed by theoretical curves calculated by numerical integration of the rate equations, eq 1 and 2, derived from Scheme II (see

$$d(\mathrm{ED})/dt = k_1(\mathrm{E})(\mathrm{A})(\mathrm{T})/[[K_{a1} + (\mathrm{A})][K_{t1} + (\mathrm{T})]] \quad (1)$$

$$d(\mathrm{ED}_2)/dt = k_2(\mathrm{ED})(\mathrm{A})(\mathrm{T})/[[K_{a2} + (\mathrm{A})][K_{t2} + (\mathrm{T})]] \quad (2)$$

Discussion). In these equations (E), (ED), and (ED$_2$) are the sums of the concentrations of enzyme species either free, (E), or bearing one adenylate, (ED), or two adenylates, (ED$_2$). The concentrations of free ATP–Mg and tryptophan are respectively (A) and (T). Analyses of stopped-flow data were performed considering different amplitudes for the fluorescence changes F_1 and F_2 related to each adenylate synthesis. The

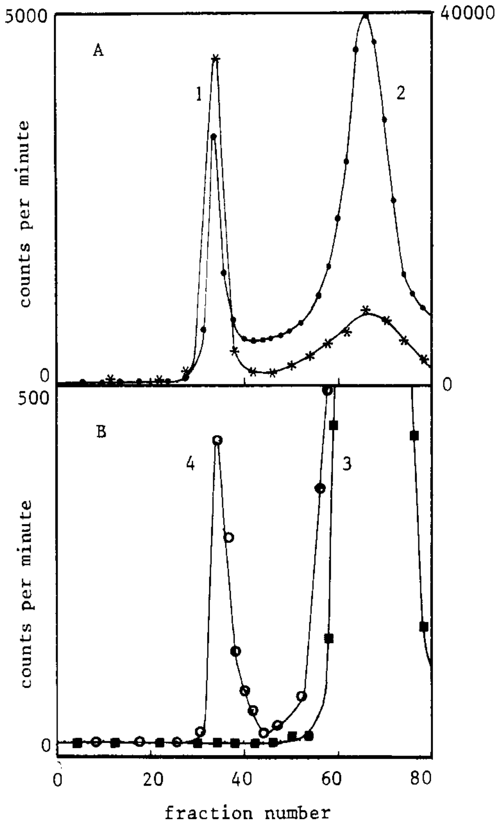

FIGURE 1: Gel filtration of *E. coli* tryptophanyl-tRNA synthetase complexes on Sephadex G-25. Tryptophanyl-tRNA synthetase (1 μM) was incubated for 5 min with 10 μM L-tryptophan and 20 μM ATP–Mg in the presence of 1 unit/mL inorganic pyrophosphatase [curves 1 (*), 2 (●), and 3 (■)] or for 30 min with 100 μM L-tryptophan and 500 μM ATP–Mg at 25 °C in standard buffer [curve 4 (○)]. L-[^{14}C]Tryptophan and [^{14}C]ATP were used for curves 1 (*) and 2 (●), respectively, and [β,γ-$^{32}P_2$]ATP was used for curves 3 (■) and 4 (○). The reaction mixture (200 μL) was filtered through the column with the standard buffer as eluent. Each collected fraction (100 μL) was treated for radioactivity determination as described under Materials and Methods. Counts per minute in panel A are represented on two scales because the specific radioactivities of the two ^{14}C labels were different: left scale, L-[^{14}C]tryptophan; right scale, [^{14}C]ATP.

value used for the ratio F_1/F_2 was the mean value coming from stopped-flow experiments carried out at constant substrate concentrations.

RESULTS

Transient Tryptophanyl Adenylate Formation. (*A*) *Stoichiometry of Tryptophanyl Adenylate Formation.* Gel filtration experiments were carried out on Sephadex G-25 in order to show the transience of tryptophanyl adenylate–enzyme complex formation and its stoichiometry in the *E. coli* system. This step is thought to precede the tryptophanyl-ATP ester synthesis evidenced by Muench (1969) and by Andrews et al. (1985). Tryptophanyl-tRNA synthetase was first incubated with ATP and tryptophan under various conditions of concentration and labeling (Table I), and the mixture was submitted to gel filtration. At low substrate concentrations, the following observations could be made: (i) the binding stoichiometry of the ligand was close to 2 mol of L-[^{14}C]tryptophan or 2 mol of [^{14}C]ATP per mole of enzyme, depending on the labeled substrate (Figure 1A); (ii) no radioactivity was eluted with the protein peak when [β,γ-$^{32}P_2$]ATP was the labeled substrate, indicating that ATP had lost its pyrophosphate moiety and that at least the adenine moiety was retained on the protein simultaneously with tryptophan. These data were in agreement with the expected formation of an enzyme–(tryptophanyl adenylate)$_2$ complex. At high substrate concentrations and after a longer reaction time, 1.2 mol of uncleaved [β,γ-$^{32}P_2$]ATP remained bound per mole of enzyme (Figure 1B and Table I). This showed that the adenylate previously retained on the enzyme had been converted into a new ATP-containing derivative. These data were in agreement with the observations by Muench (1969) and Andrews et al. (1985) that tryptophanyl-ATP ester can be synthesized by the *E. coli* enzyme and can bind to the protein.

(*B*) *Tryptophanyl Adenylate Pyrophosphorolysis.* The nature of the reaction products was checked by the following experiments: tryptophanyl-tRNA synthetase was incubated for 15 min in the presence of either low concentrations (Figure 2A) or high concentrations (Figure 2B) of ATP and L-[^{14}C]tryptophan (minute amounts of inorganic pyrophosphatase were added to the former incubation mixture in order to ensure tryptophanyl adenylate synthesis at low substrate concentrations). In each case, the mixture was split into two parts that were filtered through two Sephadex G-25 columns equilibrated with standard buffer containing no PP$_i$

Table I: Gel Filtration of Tryptophanyl-tRNA Synthetase Complexes on Sephadex G-25

conditions	label	mol of label/mol of enzyme
1 μM synthetase, 10 μM Trp, 20 μM ATP, 1 unit/mL inorganic pyrophosphatase; 5-min incubation	[^{14}C]Trp	1.9
	[^{14}C]ATP	1.7
	[β,γ-$^{32}P_2$]ATP	0
2 μM synthetase, 100 μM Trp, 500 μM ATP, 1 unit/mL inorganic pyrophosphatase; 30-min incubation	[β,γ-$^{32}P_2$]ATP	1.2

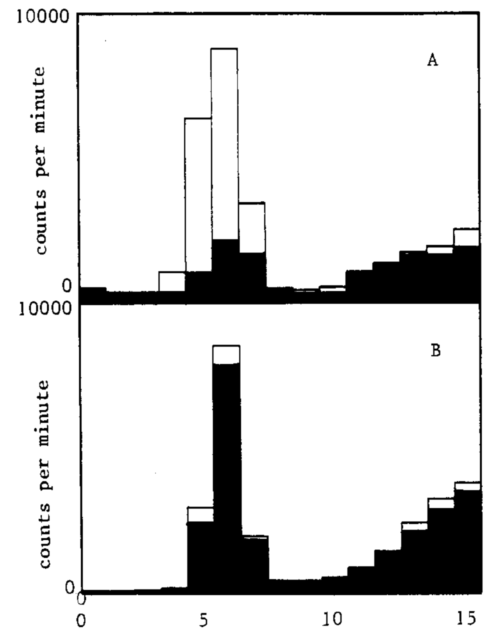

FIGURE 2: Gel filtration of *E. coli* tryptophanyl-tRNA synthetase complexes on Sephadex G-25 in the presence of inorganic pyrophosphate. Tryptophanyl-tRNA synthetase (5 μM) was incubated for 15 min at 25 °C with 20 μM L-[^{14}C]tryptophan and 20 μM ATP–Mg in the presence of 1 unit/mL inorganic pyrophosphatase (panel A) or with 50 μM L-[^{14}C]tryptophan and 2 mM ATP–Mg (panel B) in standard buffer. Aliquots (200 μL) of each solution were loaded on two identical Sephadex G-25 columns. For the first column, the standard buffer was used as eluent (open peaks); for the second column, the standard buffer containing 400 μM PP$_i$–Mg was used (filled peaks). Aliquots of the fractions were counted for radioactivity. No L-[^{14}C]tryptophan eluted with the enzyme when the incubation mixture did not contain ATP–Mg.

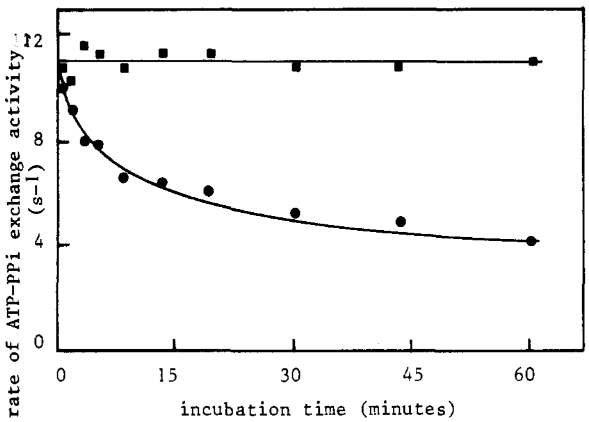

FIGURE 3: [^{32}P]PP$_i$–ATP isotopic exchange activity of *E. coli* tryptophanyl-tRNA synthetase complexes. A 200-μL aliquot of a solution in standard buffer of 1 μM tryptophanyl-tRNA synthetase, 50 μM L-tryptophan, and 2 mM ATP–Mg (●) or 200 μL of the same mixture containing 500 μM PP$_i$–Mg (■) was incubated at 25 °C. As a function of the incubation time, the [^{32}P]PP$_i$–ATP exchange activity of the enzyme was measured as follows: 10-μL aliquots of the incubation solution were removed and mixed with 490 μL of the exchange reaction mixture containing 5 μM L-tryptophan, 500 μM ATP–Mg, and 100 μM [^{32}P]PP$_i$. At time 15, 30, and 45 s, 100 μL of the reaction mixture was removed and treated as described under Materials and Methods ([^{32}P]PP$_i$ exchange kinetics).

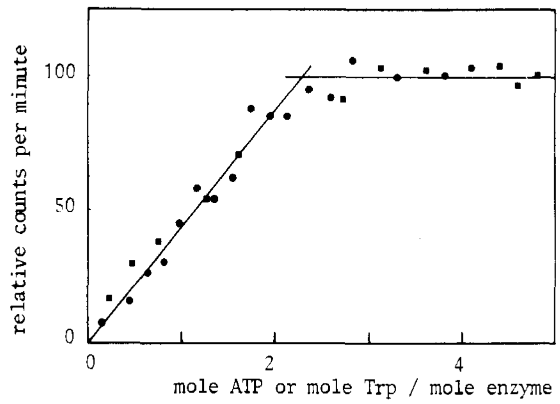

FIGURE 4: Stoichiometry of L-[^{14}C]tryptophan binding to *E. coli* tryptophanyl-tRNA synthetase in the presence of ATP–Mg. The reaction mixture contained either 2.5 μM tryptophanyl-tRNA synthetase, 100 μM ATP–Mg, 1 unit/mL inorganic pyrophosphatase, and variable L-[^{14}C]tryptophan concentrations (■) or 1 μM tryptophanyl-tRNA synthetase, 5 μM L-[^{14}C]tryptophan, 1 unit/mL inorganic pyrophosphatase, and variable ATP–Mg concentrations (●). The solution (500 μL) was incubated at 25 °C. The concentration of the variable substrate was increased stepwise by addition of 2 μL of a stock solution of the substrate. Two minutes after each addition, 10-μL aliquots of the reaction mixture were removed and absorbed on DEAE-cellulose filter disks. After washing and drying, the disks were counted for radioactivity.

or 0.4 mM PP$_i$. As previously shown, PP$_i$ cannot reverse the formation of the ester (Andrews et al., 1985). When the enzyme had been incubated with low ATP and tryptophan concentrations, the radioactivity eluted with the protein was strongly reduced in the presence of PP$_i$ (Figure 2A). This was not observed when incubating the enzyme with high substrate concentrations (Figure 2B). These results were interpreted as showing that PP$_i$ had pyrophosphorolyzed the tryptophanyl adenylate still present after the incubation period as a tight complex with the enzyme (the extent of pyrophosphorolysis in Figure 2A showed that the inorganic pyrophosphatase present in the incubation mixture did not inhibit the pyrophosphorolysis reaction at the used PP$_i$ concentration). Therefore, the radioactivity eluted with the protein peak corresponded to the ester molecules already formed at the end of the incubation period and bound to the enzyme as a complex. At high substrate concentrations, the tryptophanyl-ATP–enzyme complex had accumulated and tryptophanyl adenylate was present in very low proportion.

(*C*) *Inhibition of Tryptophanyl Adenylate Formation by Tryptophanyl-ATP Ester.* The rate of ATP–[^{32}P]PP$_i$ isotopic exchange was determined in the presence of various amounts of tryptophanyl-ATP ester. The enzyme–ester complex was preformed by incubating the enzyme with an excess of tryptophan and ATP for increasing periods of time. The isotopic exchange activity was then measured by adding an aliquot of this mixture to an exchange reaction medium. Figure 3 shows the evolution of this ATP–[^{32}P]PP$_i$ isotopic exchange activity as a function of the preincubation time. After 1 h of preincubation, the exchange activity was less than 50% of its initial value, showing that the inhibition extent of the exchange reaction followed the increase of the enzyme–ester complex concentration. In a control experiment, where the preincubation was carried out in the presence of 0.5 mM PP$_i$, there was no decrease of the exchange activity. In this latter case, PP$_i$ prevented the adenylate from being present in significant concentration and therefore prevented the formation of tryptophanyl-ATP ester.

When taken all together, the experiments shown in Figures 1–3 led to the conclusion that the ester was synthesized through an initial transient formation of tryptophanyl adenylate. Both subunits of the *E. coli* synthetase were able to catalyze these successive reactions.

Radioactivity and Fluorescence Titration. The stoichiometry of the tryptophanyl adenylate–enzyme complex was examined both by radioactive and fluorometric methods. The DEAE-cellulose filtration experiments, where ATP and tryptophan were alternately the variable or the fixed substrate and tryptophan was the labeled species, showed that below a ratio of 2 mol of ATP or tryptophan per mole of enzyme, the bound radioactivity followed a linear dependence, and beyond this value it leveled off (Figure 4). This indicated the formation of 2 mol of tryptophanyl adenylate per mole of enzyme. When ATP was added to an enzyme solution containing tryptophan and inorganic pyrophosphatase, the fluorescence intensity of the mixture decreased, due to formation of tryptophanyl-ATP, as previously noted by Andrews et al. (1985). The dependence of the fluorescence quenching was examined under increasing ATP concentrations (Figure 5). This dependence was not linear on ATP addition. This suggested that the fluorescence quenching of the enzyme subunits was not identical for each monomer and that the rate of the reaction leading to the adenylate was different on each site. The dependence of the quenching on ATP concentration was in agreement with a stoichiometry of two ATP molecules per enzyme. Beyond addition of ATP at a ratio of 2 mol of ATP per mole of enzyme, a further fluorescence quenching was noted, which was not a screening effect of ATP but rather an effect of tryptophanyl-ATP ester formation (Figure 5). The fluorescence quenching could not be related to a direct effect of ATP on the enzyme beause it did not take place in the absence of tryptophan. However, both approaches led to the conclusion that 2 mol of tryptophanyl adenylate were synthesized before ester formation took place.

Kinetic Studies of Tryptophanyl Adenylate Formation. (*A*) *[β,γ-$^{32}P_2$]ATP Depletion Experiments.* The consumption of ATP on mixing the enzyme with tryptophan and ATP in the presence of inorganic pyrophosphatase was examined under the ATP depletion conditions described by Fersht et al. (1975). In all cases, tryptophan was in excess over the enzyme. The

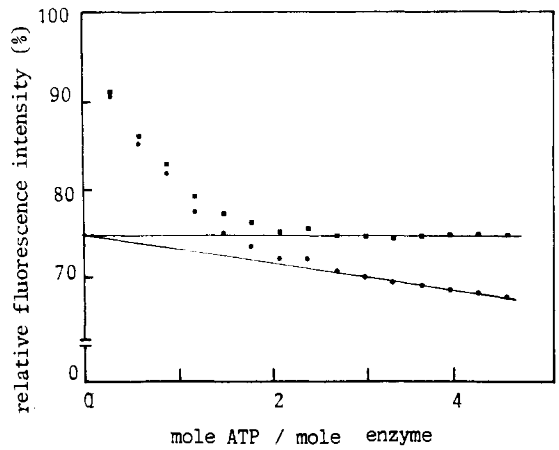

FIGURE 5: Spectrofluorometric titration of *E. coli* tryptophanyl-tRNA synthetase active sites. Fluorescence changes of the reaction mixture as a function of the ATP–Mg concentration were recorded by using an excitation wavelength of 290 nm (2-nm band-pass) and an emission wavelength of 330 nm (8-nm band-pass). Aliquots (1 μL) of a stock solution of ATP–Mg were added stepwise to 500 μL of reaction mixture containing 2.5 μM tryptophanyl-tRNA synthetase, 20 μM L-tryptophan, and 1 unit/mL inorganic pyrophosphatase in standard buffer at 25 °C. The incubation time between additions was around 90 s. (●) Experimental points recorded after ATP–Mg additions; (■) titration curve obtained after correcting the experimental points for the linear decrease of fluorescence intensity observed for ratios of ATP–Mg concentration/enzyme concentration higher than 2. It was checked that at the final concentration used, 12 μM, ATP had no screening effect.

ATP concentration ranged from 1 to 10 times the enzyme concentration. Figure 6 shows that, depending on the excess of ATP over the enzyme, different patterns could be observed. At a 10-fold excess of ATP over the enzyme (Figure 6A), there was an initial consumption of ATP close to a stoichiometry of 2 mol of ATP per mole of enzyme. This consumption was complete within 1 min. Then, a slow decrease of the residual ATP concentration occurred. This decrease, which led to total ATP disappearance, could be analyzed as a first-order process. In a series of experiments carried out at different enzyme, ATP, and tryptophan concentrations, this slow process had a rate proportional to the enzyme concentration. The stoichiometry of the ATP consumption, obtained by extrapolation to time zero of this slow phase, was 1.8 ± 0.15 mol of ATP per mole of enzyme and was in good agreement with the stoichiometry obtained by filtration or titration. When the ATP concentration was reduced to twice that of the enzyme (Figure 6B), no ATP disappearance could be observed as a slow process by contrast with the data obtained under the conditions of Figure 6A. The initial ATP depletion could be satisfactorily analyzed as a two-phase process by nonlinear regression, using a least-squares optimization (see Materials and Methods). Each of these two phases corresponded to a consumption of 1 mol of ATP per mole of enzyme. When the ATP and enzyme concentrations were equivalent, no slow phase appeared and the ATP depletion could be analyzed as a single process (Figure 6C).

In this series of ATP depletion experiments (Figure 6), three successive chemical events were observed. The first two, corresponding each to the consumption of 1 mol of ATP per dimer, could be reasonably ascribed to the formation of 1 mol of tryptophanyl adenylate per enzyme subunit. The third, corresponding to the total consumption of excess ATP, apparently reflected the formation of tryptophanyl-ATP and the further hydrolysis of this compound. This hydrolysis regenerated ATP, which could lead to new adenylate formation, with subsequent release of labeled PP_i. Scheme I, in which Ad

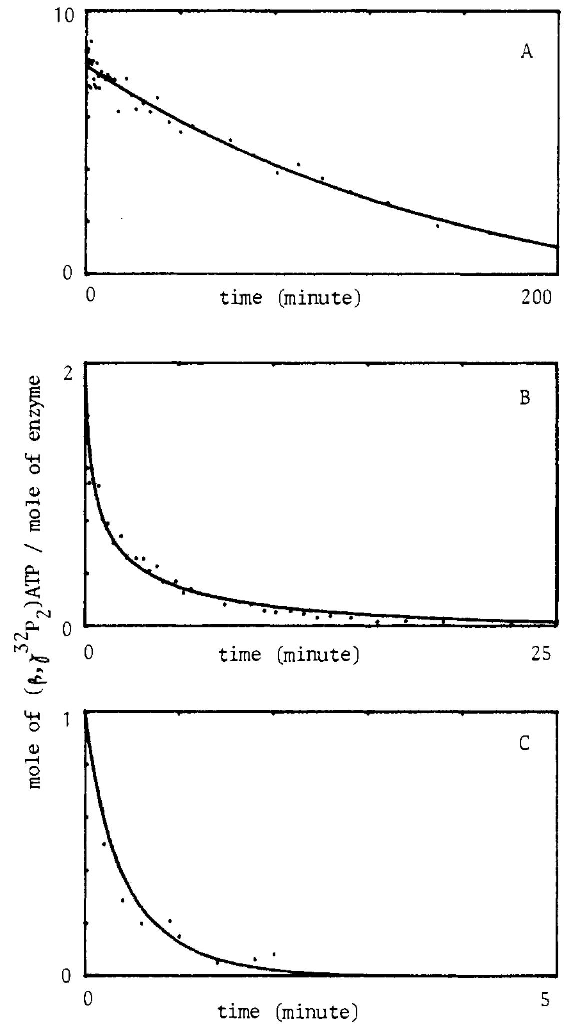

FIGURE 6: Kinetics of [β,γ-$^{32}P_2$]ATP depletion as a function of time. The experimental conditions were as follows: (A) 5 μM tryptophan, 1 μM [β,γ-$^{32}P_2$]ATP–Mg, and 0.1 μM tryptophanyl-tRNA synthetase; (B) 5 μM tryptophan, 1 μM [β,γ-$^{32}P_2$]ATP–Mg, and 0.5 μM tryptophanyl-tRNA synthetase; (C) 5 μM tryptophan, 0.5 μM [β,γ-$^{32}P_2$]ATP–Mg, and 0.5 μM tryptophanyl-tRNA synthetase. The reaction mixtures were incubated at 25 °C in standard buffer with 0.1 unit/mL inorganic pyrophosphatase. Aliquots were removed as a function of time and treated for [β,γ-$^{32}P_2$]ATP radioactivity determination as described under Materials and Methods. In (A), the slow consumption of [β,γ-$^{32}P_2$]ATP was exponential. The time constant of the exponential was 0.006 min^{-1}, and its amplitude corresponded to 8.14 mol of ATP consumed per mole of enzyme. This indicated that 1.86 mol of ATP–Mg per mole of enzyme were consumed in a fast process. In (B) and (C), the complete consumption of ATP has been fitted by using the nonlinear regression described under Materials and Methods. The curves that fit the points correspond to the following parameter values: k_1 = 150 s^{-1}, k_2 = 3 s^{-1}, K_{t1} = 25 μM, K_{t2} = 5 μM, K_{a1} = 200 μM, and K_{a2} = 100 μM.

Scheme I

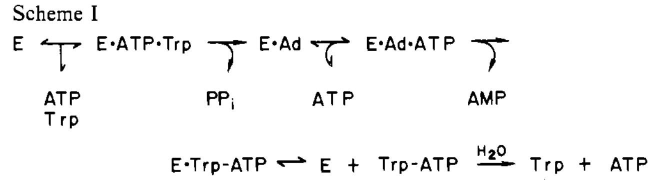

stands for tryptophanyl adenylate and Trp-ATP for tryptophanyl-ATP ester, summarizes these successive reactions.

(*B*) *Stopped-Flow Analysis of Tryptophanyl Adenylate Formation.* The study of the three processes evidenced in the ATP depletion experiments was carried out by the stopped-flow method, using the fluorescence decrease observed after mixing the enzyme with tryptophan and ATP in the fluorescence

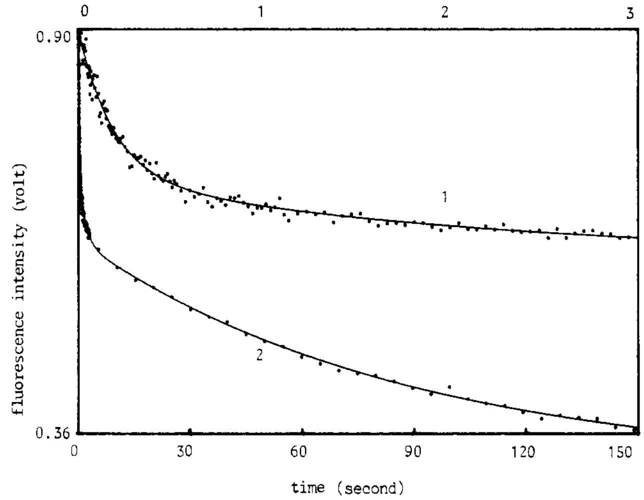

FIGURE 7: Stopped-flow fluorescence change of an *E. coli* tryptophanyl-tRNA synthetase solution under conditions of tryptophanyl adenylate synthesis. Conditions were as follows: 0.2 μM tryptophanyl-tRNA synthetase, 5 μM L-tryptophan, 50 μM ATP–Mg, and 0.2 unit/mL inorganic pyrophosphatase in standard buffer at 25 °C. Rise time was 1 ms. Curve 1, upper time scale; curve 2, lower time scale. Fitting of the data was performed with the function $F = A_1 \exp(-k_1t) + A_2 \exp(-k_2t) + A_3 \exp(-k_3t) + A_4$. The values found for the parameters were $k_1 = 5.43$ s^{-1}, $k_2 = 0.584$ s^{-1}, $k_3 = 0.0116$ s^{-1}, $A_1 = 0.192$ V, $A_2 = 0.088$ V, $A_3 = 0.301$ V, and $A_4 = 0.316$ V.

titration experiments (Figure 5). Two sets of conditions were used: either a large excess or both tryptophan and ATP or a slight excess of one of them over the enzyme. In the latter case, the limiting substrate concentration largely decreased during the chemical reactions.

When *E. coli* tryptophanyl-tRNA synthetase was mixed with a large excess of ATP and tryptophan, the fluorescence decrease was triphasic (Figure 7). This was observed whatever the concentrations of both substrates were. The three phases had very different rates, and particularly the third phase was much slower than the first two ones. This third phase could be separately analyzed as a first-order process. Its time constant was ATP concentration dependent and was not tryptophan concentration dependent. The apparent K_m for ATP was 40 ± 15 μM, and the maximum rate constant of this third phase was 0.025 ± 0.005 s^{-1}. The analysis of the fluorescence decay related to the first two phases was then carried out by considering this decay as the sum of two exponentials, after subtraction of the fluorescence quenching due to the third phase. The rate dependence of each phase on ATP and tryptophan concentrations gave linear double-reciprocal plots (Figure 8), from which one could conclude that there was no synergy between ATP and tryptophan binding. The maximum rate constants related to the first and to the second phases were respectively k_1 = 146 ± 17 s^{-1} and k_2 = 3.3 ± 0.9 s^{-1}. The Michaelis constants for ATP and tryptophan were respectively as follows: K_{a1} = 179 ± 35 μM (first phase) and K_{a2} = 116 ± 45 μM (second phase); K_{t1} = 23.9 ± 7.9 μM (first phase) and K_{t2} = 3.7 ± 2.2 μM (second phase). The kinetic parameters of the second process were less accurately determined because the second phase was overlapped by the end of the first phase and by the beginning of the third one. The amplitude was notably smaller for the second exponential phenomenon than for the two others.

Under conditions of substrate depletion, two fast phases followed by a slower one were observed as under constant substrate concentration (Figure 9). The third phase behaved as an exponential, as previously, and the analysis of the first two phases could be carried out as described by Merle et al. (1984) using nonlinear regression procedures. These analyses gave rate constants in agreement with those determined at constant substrate concentrations for the two fast phases. The relative amplitude of the fluorescence decrease of the third phase represented a large fraction of the total fluorescence variation, even when the tryptophan concentration was only in slight excess over that of the enzyme subunits, as in Figure

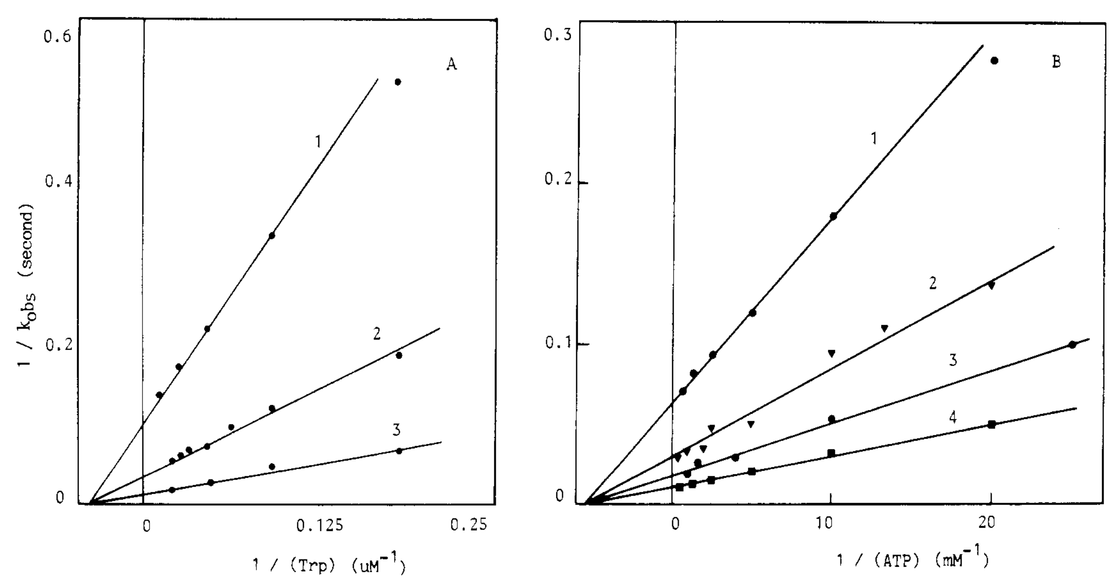

FIGURE 8: Analysis of the dependence of the rate constant of the first kinetic phase of tryptophan adenylation on L-tryptophan and ATP–Mg concentration. (A) Plot of the reciprocal of the time constant as a function of the reciprocal of L-tryptophan concentration. Three sets of experiments were performed with three different ATP–Mg concentrations: 12.5, 50, 200 μM in plots 1, 2, and 3, respectively. The enzyme concentration was in the range 0.1–0.8 μM. Each set of experiments was analyzed independently by fitting the points with a hyperbolic regression program: $k_{obs} = k_{max}(S)/[K_m + (S)]$ with (S) = substrate concentration and K_m = Michaelis constant. The calculated values were as follows: K_m(Trp) = K_{t1} = 22.8 ± 5.2, 22.7 ± 6.4, and 26.3 ± 7.5 μM; k_{max} = 9.65 ± 1.85, 26.3 ± 4.2, and 81.0 ± 16.4 s^{-1} in plots 1, 2, and 3, respectively. (B) Plot of the reciprocal of the time constant as a function of the reciprocal of ATP–Mg concentration. Four sets of experiments were carried out with L-tryptophan concentrations of 3, 6, 15, and 50 μM and enzyme concentrations of 0.25, 0.3, 0.4, and 1 μM in plots 1, 2, 3, and 4, respectively. By use of the same procedure for data analysis, the following values were calculated: K_m(ATP–Mg) = K_{a1} = 166 ± 10, 180 ± 35, 178 ± 41, and 192 ± 38 μM; k_{max} = 15.1 ± 0.3, 28.3 ± 5.3, 54.1 ± 5.3, and 96.1 ± 8.0 s^{-1} in plots 1, 2, 3, and 4, respectively. The straight lines on the diagram have been plotted by using the mean K_m values: K_{t1} = 23.9 ± 7.9 μM and K_{a1} = 179 ± 35 μM.

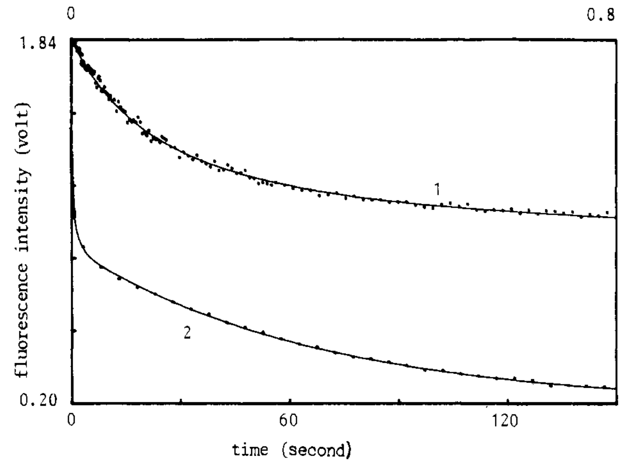

FIGURE 9: Stopped-flow fluorescence change for the formation of *E. coli* tryptophanyl-tRNA synthetase–tryptophanyl adenylate complex under tryptophan depletion conditions. The reaction mixture contained 0.75 μM tryptophanyl-tRNA synthetase, 2 μM L-tryptophan, 200 μM ATP–Mg, and 0.1 unit/mL inorganic pyrophosphatase. Five experiments were averaged; rise time was 5 ms. The fluorescence change of the solution is represented according to two time scales: curve 1, upper time scale, and curve 2, lower time scale. The final slow phase was analyzed as a monoexponential function with a time constant equal to 0.015 s^{-1} and an amplitude equal to 0.70 V. The fast fluorescence decrease was analyzed by using the iterative procedure based on Scheme II (see Materials and Methods). The curve that fit the points corresponded to the following values for the kinetic parameters: k_1/K_{a1} = 1.0 s^{-1} μM^{-1}, k_2/K_{a2} = 4.1 × 10^{-2} s^{-1} μM^{-1}, K_{t1} = 23 μM, and K_{t2} = 3.0 μM. The amplitude of fluorescence changes related to the first and second tryptophanyl adenylate synthesis were 0.70 and 0.23 V, respectively.

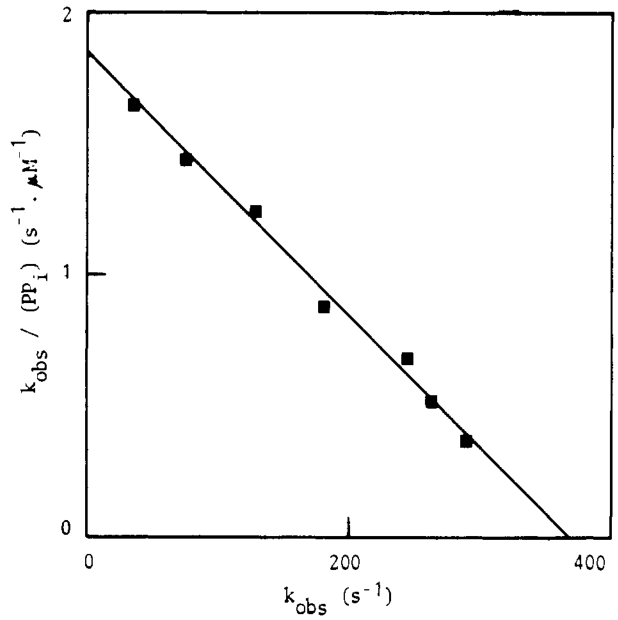

FIGURE 10: Analysis of the dependence of the adenylate pyrophosphorolysis rate constant on PP_i–Mg concentration. Stopped-flow experiments were done, starting from a tryptophanyl adenylate–tryptophanyl-tRNA synthetase complex preformed by incubating for 5 min at 25 °C 2 μM enzyme, 5 μM tryptophan, 20 μM ATP–Mg, and 0.5 unit/mL inorganic pyrophosphatase as described under Materials and Methods. The increase of the fluorescence intensity was analyzed as a monoexponential function at all PP_i concentrations. The figure represents the Eadie plot of the dependence of the time constant on PP_i–Mg concentration. The value of K_m was 196 ± 12 μM, and the value of K_b was 360 ± 10 s^{-1}.

9. This was surprising if the third phase reflected the quenching of the tryptophan molecule engaged in the tryptophanyl-ATP ester. Indeed, the quenching related to the first two phases was nearly equivalent to half the initial fluorescence intensity of the enzyme. At an equal concentration, the fluorescence intensity of free tryptophan is only 6% of the fluorescence intensity of the enzyme (Andrews et al., 1985). Consequently, the quenching related to all three phases was mostly related to conformation changes of the enzyme and not to a change of the substrate tryptophan. In the particular case of the third phase, the fluorescence quenching coincided with the synthesis of the tryptophanyl-ATP ester but did not directly reflect the accumulation of this derivative under limiting tryptophan concentration.

Kinetic Study of Tryptophanyl Adenylate Pyrophosphorolysis. On the basis of the previous data the initial reaction product obtained after mixing enzyme, ATP, and tryptophan was tryptophanyl adenylate. It was rapidly formed and then slowly converted into tryptophanyl-ATP ester. When PP_i was added within a very few minutes after mixing the enzyme with a slight excess of tryptophan and ATP in the presence of inorganic pyrophosphatase, the adenylate formation was reversed. When such experiments were carried out in the stopped-flow apparatus, single exponentials were obtained at all PP_i concentrations used, a fact suggesting that the reversal of the synthesis of the two adenylates had occurred with the same rate in a simple Michaelian way, in contrast to the adenylate formation. The rate and Michaelis constants for the pyrophosphorolysis reaction, deduced from the Eadie plot (Figure 10), were k_b = 360 ± 10 s^{-1} and K_P = 196 ± 12 μM.

Discussion

The product isolated by gel filtration, after reaction of *E. coli* tryptophanyl-tRNA synthetase with ATP and tryptophan, was described as the tryptophanyl-ATP ester (Muench, 1969), a product resembling the aminoacyl-tRNA by the presence of an ester linkage between the amino acid carboxyl and the ribose hydroxyl groups of ATP. The expected aminoacyl adenylate was not isolated. Two questions could be raised. (i) Does tryptophanyl adenylate form in significant amounts in the absence of an amino acid acceptor, as in the case for a series of synthetases requiring tRNA as a necessary participant to the amino acid activation [arginyl- (Mitra & Mehler, 1966; Fersht et al., 1978), glutaminyl- (Revel et al., 1965; Kern et al., 1980), and glutamyl- (Kern & Lapointe, 1981) tRNA synthetases]? In the present case, ATP would be such a pseudoacceptor, leading to tryptophanyl-ATP as a nonphysiological byproduct in the absence of tRNA. (ii) Are the fast fluorescence changes linked to the addition of ATP and tryptophan to the enzyme significant of tryptophanyl adenylate formation and are both subunits equivalent?

The data obtained by gel filtration show that a compound containing tryptophan and adenine migrates with the enzyme before tryptophanyl-ATP is synthesized. This compound gives rise to resynthesis of ATP in the presence of PP_i, even in the absence of added AMP. Because an adenyl-enzyme has been ruled out as a kinetic intermediate in the ATP–[^{32}P]PP_i exchange (Lowe & Tansley, 1984; Conolly et al., 1984), the initial derivative observed in the present experiments can only be the aminoacyl adenylate. The stoichiometry of tryptophanyl adenylate formation, 1.8–2 per dimeric enzyme, indicates that both subunits are able to carry out the synthesis of this derivative, as observed for the homologous beef enzyme.

There are three distinct kinetic processes. The ATP depletion data show that, at low ATP concentration, 2 mol of ATP are consumed per mole of enzyme within a few minutes, in two different phases. Gel filtration data show that, during the same period, 2 mol of tryptophanyl adenylate are syn-

Scheme II

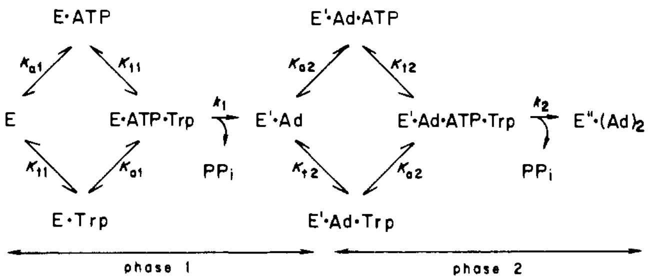

thesized on the enzyme. This allows us to assign the synthesis of one adenylate per phase, and it can be assumed that the first two phases of the stopped-flow experiments also represent the formation of two adenylates with quite different rate constants. When these stopped-flow experiments are carried out under conditions of constant substrate concentrations, the rates of the first two phases are dependent on ATP and tryptophan concentrations, as expected for tryptophanyl adenylate formation. Two Michaelis constants for tryptophan can be deduced, the value for the second phase being smaller (Table II). However, equilibrium data have led to a single value for the dissociation constant of tryptophan: 120 μM for each site in the absence of ATP (Muench, 1976). This discrepancy may only be partly explained by the different experimental conditions used for the binding experiments, pH 6.9 and 3 °C, compared to our conditions, pH 8 and 25 °C. The large fluorescence quenching associated with the first tryptophanyl adenylate formation implies a structural rearrangement of the protein. Such a rearrangement is likely the reason for the improved binding of tryptophan on the site forming the second tryptophanyl adenylate. This leads to the conclusion that the adenylate formation on the second reacting subunit is dependent on the adenylate synthesis on the first reacting subunit and that it occurs only after this first process. These assumptions are summarized by Scheme II, where E, E′, and E″ denote different enzyme conformations and Ad stands for tryptophanyl adenylate. The Michaelis constants for ATP and tryptophan relative to phases 1 and 2 are respectively K_{a1}, K_{a2}, K_{t1}, and K_{t2} and refer to the overall process corresponding to each phase. The rate constants of tryptophan activation are k_1 and k_2.

This model was used to analyze the first two phases of the [β,γ-$^{32}P_2$]ATP depletion and of the stopped-flow data at low ATP and tryptophan concentrations. It was not possible to obtain a good fit when Scheme II was replaced by a model in which both sites could work simultaneously. The best fit obtained by numerical integration, using the binding constants obtained from the stopped-flow data, gave rate constants in agreement with those coming from the stopped-flow data analysis. This is strong evidence that the two fast processes seen by these two techniques are the same and represent the successive syntheses of two molecules of tryptophanyl adenylate, one on each enzyme subunit. At substrate saturation, the ratio between the maximum activities of tryptophanyl adenylate synthesis on both sites, k_1/k_2, has the large value of 150/3 = 50. Such a ratio corresponds nearly to a half-of-the-sites reactivity, a behavior that has also been observed for tyrosyl-tRNA synthetase from *B. stearothermophilus* (Fersht, 1975). Although this later synthetase binds only 1 mol of tyrosine and 1 mol of tyrosyl adenylate per mole of enzyme, there is a second set of binding sites for tyrosine and ATP which becomes accessible when the first site is occupied with tyrosyl adenylate (Fersht, 1975). For the *E. coli* tryptophanyl-tRNA synthetase, at substrate concentrations well below the Michaelis constants, the ratio k_1/k_2 is reduced to $(k_1/k_2)(K_{a2}K_{t2}/K_{a1}K_{t1}) = 5$, a figure implying that the activity of the second site becomes comparatively more significant. This may reflect an adaptative way of the bacteria to withstand a lowering of its nutrients.

The third phase seen through the [β,γ-$^{32}P_2$]ATP depletion experiments led to total ATP disappearance and was first ordered whatever the excess of ATP over the enzyme. Its time constant was enzyme concentration dependent. The [β,γ-$^{32}P_2$]ATP consumption is directly linked to tryptophanyl adenylate synthesis. Several hypotheses could account for the appearance of a slow turnover of tryptophanyl adenylate synthesis. This slow turnover could be due either to the adenylate hydrolysis, to tryptophanyl-Tris amide synthesis (Andrews et al., 1985), or to the ester formation. A limiting adenylate hydrolysis or aminolysis would generate a zero-ordered process, which is not the case. Furthermore, the tryptophanyl-Tris amide formation is very slow. It seems therefore that the limiting process is essentially the ester synthesis, followed by its nonenzymatic hydrolysis (Andrews et al., 1985).

When the stopped-flow experiments were carried out under limiting tryptophan concentration conditions, the amplitude of the third phase was of the same order of magnitude as the sum of the amplitudes of the first two phases (Figure 9). Considering the relative concentration of tryptophan and of the enzyme in these experiments, the amplitude of the third phase reflects mainly a conformational change of the enzyme linked to the ester formation. Analysis of the experiments carried out under limiting ATP concentration conditions leads to the same conclusion. This suggests that the enzyme undergoes a further conformational change after the second tryptophanyl adenylate formation. This change occurs at a maximum rate constant of 0.025 s^{-1}, which is comparable to the rate of ester formation obtained by thin-layer chromatography data, 0.017 s^{-1} (Andrews et al., 1985). Consequently, the synthesis of tryptophanyl-ATP ester is probably dependent on this structural rearrangement. A conformational change is also known to be brought about by the presence of $tRNA^{Phe}$ lacking its CCA end for phenylalanyl-tRNA synthetase, an enzyme that is able to aminoacylate AMP in the presence of this incomplete tRNA (Renaud et al., 1981). The observed conformational change is in agreement with the crystallographic data on *B. stearothermophilus* tryptophanyl-tRNA synthetase (Carter & Carter, 1979), an enzyme closely related to the *E. coli* synthetase as judged from sequence data (Hall et al., 1982). This enzyme presents different crystal forms, depending on whether it is free or complexed with tryptophanyl-ATP ester.

Contrasted Behaviors between E. coli and Beef Tryptophanyl-tRNA Synthetases. Table II summarizes the data obtained for the procaryotic and the eucaryotic enzymes. Several opposite properties between the two enzymes can be underlined: (i) during the adenylation process, both subunits of the beef enzyme are identically active at substrate saturation while one subunit of the *E. coli* enzyme is nearly inactive when compared to the other; (ii) in the beef system, there is anticooperative binding of tryptophan to the two subunits, either in the absence or in the presence of ATP, while in the *E. coli* system the two subunits have the same affinity for tryptophan in the absence of ATP (Muench, 1969) and show a positive cooperativity of kinetic origin, in the presence of ATP; (iii) the beef enzyme has no apparent ability to synthesize tryptophan derivatives such as tryptophanamide while the *E. coli* enzyme can perform such syntheses (Andrews et al., 1985); (iv) a large fluorescence change linked to tryptophanyl-ATP

Table II: Comparison between Tryptophanyl-tRNA Synthetases from *E. coli* and Beef Pancreas

		tryptophanyl-tRNA synthetase	
		E. coli	beef
$M_r \times 10^{-3}$		74[a]	108–120[b]
tryptophanyl adenylate synthesis	k_1 (s^{-1})	146 ± 17[c]	42 ± 3[d]
	k_2 (s^{-1})	3.3 ± 0.9[c]	42 ± 3[d]
	K_{a1} (μM)	179 ± 35[c]	1400 ± 100[d]
	K_{a2} (μM)	116 ± 45[c]	1400 ± 100[d]
	K_{t1} (μM)	23.9 ± 7.9[c]	1.6 ± 0.3[d]
	K_{t2} (μM)	3.7 ± 2.2[c]	18.5 ± 1.5[d]
tryptophanyl adenylate pyrophosphorolysis	k_b (s^{-1})	360 ± 10[c]	190 ± 10[e]
	K_P (μM)	196 ± 12[c]	290 ± 40[e]
tryptophanyl-ATP ester synthesis	$k \times 10^3$ (s^{-1})	25 ± 5[c]	nd[j]
	K_{ATP} (μM)	40 ± 15[c]	nd[j]
tryptophanamide synthesis	k (s^{-1})	0.1[f]	none[g]
	K_{NH_3} (μM)	1000[f]	none[g]
$tRNA^{Trp}_{beef}$ aminoacylation	k (s^{-1})	0[g]	5.4[h]
$tRNA^{Trp}_{E. coli}$ aminoacylation	k (s^{-1})	8.4[i]	0.003[h]
cooperativity for Trp binding		positive	negative

[a] Hall et al., 1982. [b] Lemaire et al., 1969; Favorova et al., 1974. [c] This work. [d] Merle et al., 1984. [e] Mazat et al., 1982. [f] Andrews et al., 1985. [g] Merle, unpublished data. [h] Dorizzi et al., 1977. [i] Muench, 1976. [j] nd, not determined.

ester formation follows the tryptophanyl adenylate synthesis with the *E. coli* enzyme whereas no such change is observed for the beef enzyme; (v) each of the two enzymes is inefficient in the aminoacylation of the heterologous $tRNA^{Trp}$; (vi) there is no cross-reactivity between the *E. coli* enzyme and antibodies raised against the beef enzyme (Salafranque and Trezeguet, unpublished data), suggesting few common structural features; (vii) the molecular weights of the procaryotic and eucaryotic enzymes are quite different, suggesting also that these two homologous synthetases have structural differences. Whether all these differences are related to completely different primary and tertiary structures of the two proteins will not be known until the elucidation of the primary structure of the beef enzyme and the tertiary structure of these synthetases.

Acknowledgments

We are grateful to Dr. J. Labouesse for helpful criticism.

Registry No. ATP, 56-65-5; ATP-Mg, 1476-84-2; PP_i, 14000-31-8; tryptophanyl-ATP, 26847-97-2; tryptophanyl-tRNA synthetase, 9023-44-3; tryptophanyl adenylate, 29282-54-0; tryptophan, 73-22-3.

References

Andrews, D., Trezeguet, V., Merle, M., Graves, P. V., Muench, K. H., & Labouesse, B. (1985) *Eur. J. Biochem. 146*, 201–209.

Atkinson, T., Banks, G. T., Bruton, C. J., Comer, M. J., Jakes, R., Kalmagharan, T., Whitakee, A. R., & Winter, G. P. (1979) *J. Appl. Biochem. 1*, 247–258.

Carter, C. W., & Carter, C. W., Jr. (1979) *J. Biol. Chem. 254*, 12219–12223.

Coleman, D. E., & Carter, C. W., Jr. (1984) *Biochemistry 23*, 381–385.

Connolly, B. A., Eckstein, F., & Grotjahn, L. (1984) *Biochemistry 23*, 2026–2031.

Dorizzi, M., Labouesse, B., & Labouesse, J. (1971) *Eur. J. Biochem. 19*, 563–572.

Epely, S., Gros, C., Labouesse, J., & Lemaire, G. (1976) *Eur. J. Biochem. 61*, 139–146.

Favorova, O. O., Kochkina, L. L., Shajko, M., Parin, A. V., Khilko, S. N., Prasolov, V., & Kisselev, L. L. (1974) *Mol. Biol. (Moscow) 8*, 580–590.

Fersht, A. R. (1975) *Biochemistry 14*, 5–12.

Fersht, A. R., Ashford, J. D., Bruton, C. J., Jakes, R., Koch, G. L. E., & Hartley, B. S. (1975) *Biochemistry 14*, 1–4.

Fersht, A. R., Gangloff, J., & Dirheimer, G. (1978) *Biochemistry 17*, 3740–3746.

Graves, P. V., Mazat, J. P., Juguelin, H., Labouesse, J., & Labouesse, B. (1979) *Eur. J. Biochem. 96*, 509–518.

Graves, P. V., de Bony, J., Mazat, J. P., & Labouesse, B. (1980) *Biochimie 62*, 33–41.

Gros, C., Lemaire, G., van Rapenbusch, R., & Labouesse, B. (1972) *J. Biol. Chem. 247*, 2031–2043.

Hall, C. V., van Cleemput, M., Muench, K. H., & Yanofsky, C. (1982) *J. Biol. Chem. 257*, 6132–6136.

Joseph, D. R., & Muench, K. H. (1971) *J. Biol. Chem. 246*, 7602–7615.

Kern, D., & Lapointe, J. (1981) *Eur. J. Biochem. 115*, 29–38.

Kern, D., Potier, S., Lapointe, J., & Boulanger, Y. (1980) *Biochim. Biophys. Acta 607*, 65–80.

Kisselev, L. L., Favorova, O. O., & Kovaleva, G. K. (1979) *Methods Enzymol. 59*, 234–257.

Lemaire, G., van Rapenbusch, R., Gros, C., & Labouesse, B. (1969) *Eur. J. Biochem. 10*, 336–344.

Lemaire, G., Gros, C., Epely, S., Kaminski, M., & Labouesse, B. (1975) *Eur. J. Biochem. 51*, 237–252.

Lowe, G., & Tansley, G. (1984) *Eur. J. Biochem. 138*, 597–602.

Mazat, J. P., Merle, M., Graves, P. V., Merault, G., Gandar, J. C., & Labouesse, B. (1982) *Eur. J. Biochem. 128*, 389–398.

Merault, G., Graves, P. V., Labouesse, B., & Labouesse, J. (1978) *Eur. J. Biochem. 87*, 541–550.

Merle, M., Graves, P. V., & Labouesse, B. (1984) *Biochemistry 23*, 1716–1723.

Mitra, S. K., & Mehler, A. H. (1966) *J. Biol. Chem. 241*, 5161–5164.

Muench, K. H. (1969) *Biochemistry 8*, 4872–4879.

Muench, K. H. (1976) *J. Biol. Chem. 251*, 5195–5199.

Prasolov, V. S., Favorova, O. O., Margulis, G. V., & Kisselev, L. L. (1975) *Biochim. Biophys. Acta 378*, 92–106.

Ravel, J., Wang, S. F., Heinemeyer, C., & Shive, W. (1965) *J. Biol. Chem. 240*, 432–438.

Renaud, M., Bacha, H., Remy, P., & Ebel, J. P. (1981) *Proc. Natl. Acad. Sci. U.S.A. 78*, 1606–1608.

Scheinker, V. S., Beresten, S. F., Degtyarev, S. K., & Kisselev, L. L. (1979) *Nucleic Acids Res. 7*, 625–637.

Weiss, S. B., Zachau, H. G., & Lipmann, F. (1959) *Arch. Biochem. Biophys. 83*, 101–105.

Winter, G. P., & Hartley, B. S. (1977) *FEBS Lett. 80*, 340–342.